PAPER

Stability of icosahedral quasicrystals in a simple model with two-length scales

IOP Publishing Journal of Physics: Condensed Matter

J. Phys.: Condens. Matter **29** (2017) 124003 (10pp) doi:10.1088/1361-648X/aa586b

Stability of icosahedral quasicrystals in a simple model with two-length scales

Kai Jiang[1], Pingwen Zhang[2] and An-Chang Shi[3]

[1] School of Mathematics and Computational Science, Xiangtan University, Xiangtan 411105, People's Republic of China
[2] LMAM, CAPT and School of Mathematical Sciences, Peking University, Beijing 100871, People's Republic of China
[3] Department of Physics & Astronomy, McMaster University, Hamilton, Ontario, L8S 4M1, Canada

E-mail: kaijiang@xtu.edu.cn, pzhang@pku.edu.cn and shi@mcmaster.ca

Received 26 October 2016, revised 5 January 2017
Accepted for publication 10 January 2017
Published 13 February 2017

Abstract

The phase behaviour of a free energy functional with two length scales is examined by comparing the free energy of different candidate phases including three-dimensional icosahedral quasicrystals. Accurate free energy of the quasicrystals has been obtained using the recently developed projection method. The results reveal that the icosahedral quasicrystal and body-centred-cubic spherical phase are the stable ordered phases of the model. Furthermore, the difference between the results obtained from the projection method and the one-mode approximation has been analyzed in detail. The present study extends previous results on two-dimensional systems, demonstrating that the interactions between density waves at two length scales can stabilize two- and three-dimensional quasicrystals.

Keywords: icosahedral quasicrystals, two length scales with golden ratio, projection method

(Some figures may appear in colour only in the online journal)

1. Introduction

Crystals and quasicrystals are ordered materials with discrete Fourier spectra. Because of their translational and orientational order, the Fourier spectra of crystals form a periodic lattices in the reciprocal space. On the other hand, the quasicrystals do not possess translational order but have orientational order, i.e. quasicrystals are characterized by quasiperiodic positional order and long-range orientational order. As a result of these features, the Fourier spectra of quasicrystals are dense discrete points in the reciprocal space. Because of the decay of the Fourier coefficients, in practice, only the most intense diffractions can be observed. Although the mathematical description of quasilattices was given by Meyer in early 70 s [1], the first quasicrystal was discovered by Shechtman in Al-Mn alloys in 1982 [2]. Since then more than a hundred different metallic alloys have been found to exhibit quasicrystalline order [3, 4]. Besides hard materials such as metallic alloys, quasicrystalline order has been observed in many soft condensed matter systems, including micelle-forming liquid crystals [5–7], block copolymers [8–10], colloidal suspensions [11] and binary mixtures of nanoparticles [12].

The dimensionality of quasicrystals is determined by the lack of translational symmetry in different directions. Quasicrystals can be quasiperiodic in all three spatial dimensions, usually with icosahedral symmetry; or they can be quasiperiodic in two or one directions, and periodic in the other directions, forming two or one dimensional quasicrystals. Due to the efforts of a large number of researchers since the discovery of quasicrystals in early 80 s, the structure of quasicrystals, i.e. the distribution of atomic positions and the symmetry of the system are now well understood [13, 14]. One particularly elegant description of quasicrystals is that quasicrystalline structures can be regarded as the projection from a higher-dimensional periodic structure [1, 15]. Compared with the studies of the structure of quasicrystals, the study of the thermodynamic stability of quasicrystals remains a challenge [16, 17], largely due to the requirement of obtaining accurate free energy of the systems.

Theoretical approaches to investigating the stability of an ordered phase, including periodic and quasiperiodic

structures, often involve minimizing an appropriate free energy functional of the system. The solutions of such a minimization problem provide a set of candidate phases of the system. A comparison of the free energy of different candidate structures can then be used to construct the phase diagram of the model system. Furthermore, the availability of the solutions corresponding to different ordered phases provides insight about the mechanism of the formation of these structures. Therefore, a systematic examination of the stability of quasicrystals requires the availability of suitable free energy functionals and accurate methods to compute the free energy of phases with quasicrystalline order. A large number of phenomenological theories based on various coarse-grained free energy functionals have been proposed to study phases and phase transitions of ordered systems. The utilization of such coarse-grained density functional theories provides an effective and efficient method to investigate the phase behaviour of physical systems, especially soft matter, exhibiting ordered phases including quasicrystals. One example of such a free energy functional is the theory developed by Leibler [18], which provides useful insight and a rather accurate description of the ordered phases of diblock copolymers. Similarly, a number of coarse-grained free energy functionals have been proposed to explore the quasicrystalline order arising from model systems with more than one characteristic length scale [19–27]. The generic feature of these models is the introduction of a mechanism involving nonlinear interactions between density waves at two length scales, which can stabilize quasicrystalline order. On the other hand, most of these coarse-grained free energy functional are developed to study the emergence and stability of two-dimensional (2D) quasicrystals, including metastable octagonal quasicrystal, and stable 10-, and 12-fold symmetric quasicrystals [28]. Very recently, Subramanian *et al* [29] have shown that the three-dimensional (3D) icosahedral quasicrystal can become an equilibrium stable structure in a phase field model. The mechanism of the 3D model is similar to those 2D models with two-length-scale interaction potentials but designed in a more sophisticated way. In the present study we will focus on a minimal model which can promote the formation and stability of the 3D icosahedral quasicrystals.

Besides the availability of a proper free energy functional of the system, examining the thermodynamic stability of quasicrystals requires accurate and efficient methods to compute the free energy of different ordered phases. Because of the spatial periodicity, the computation of the free energy of crystals can be carried out within a unit cell with periodic boundary conditions. On the other hand, quasicrystals are space-filling ordered structures without spatial periodicity, thus it is not possible to reduce the structure of a quasicrystal to unit cells. In the literature, a commonly used method to overcome this difficulty is to utilize periodic structures with large unit cells to approximate the quasicrystals [21, 29–34]. The free energy computed from these quasicrystal-approximants is used as approximate values of that for quasicrystals. Mathematically, the quasicrystal approximants approach can be considered as a Diophantine approximation problem, involving the approximation of irrational numbers by rational or integer numbers. It has been shown that a gap between the free energy of the quasicrystals and their corresponding approximants always persists [1]. An example of this mathematical feature is demonstrated in the 2D dodecagonal quasicrystal and its approximant within the Lifshitz–Petrich model [35].

An alternative approach to calculate the free energy of quasicrystals is based on the observation that quasiperiodic lattices can be generated by a cut-and-project method from higher-dimensional periodic lattices. This method, initially proposed by Meyer in the study of the most periodic function in terms of the model set or Meyer set [1], provides a basic framework to investigate the quasicrystals. In particular, the cut-and-project method projects the higher-dimensional periodic lattice points within a stripe onto a lower-dimensional space to obtain the quasi-lattices or quasicrystals. This cut-and-project method is an approach to generate spatial positions of the hard (discrete) quasicrystals. Along this line, an approximate method, the Gaussian method, has been developed to study quasicrystals. The essence of the Gaussian method is that the density profile of a quasicrystal is assumed to be a sum of Gaussian functions centered at the lattice points of a predetermined quasicrystalline lattice [36]. The width of the Gaussian functions is treated as a variational parameter, which is optimized to minimize the free energy of the system. For soft (continuous) quasicrystals, there are large overlaps between the peaks of the density profiles. Therefore, they are different from the hard quasicrystals, and the Gaussian method does not provide an accurate description of soft quasicrystals. In order to study the continuous distributed quasicrystals, we proposed a generalized spectral method, the *projection method* for the computation of the continuous density profile and the free energy of quasiperiodic structures [35]. The projection method approximates a quasiperiodic (or almost periodic) function by a trigonometric polynomial defined on the whole space [1]. The expansion coefficients are computed in the higher-dimensional periodic domain. Therefore, the projection method is more suited to studying the soft quasicrystals. In our previous studies it has been demonstrated that the projection method can be used to obtain the equilibrium density profile of quasicrystals and evaluate their energy densities to high accuracy [28, 35].

In the present work, we apply the projection method to study the relative stability of different ordered phases in a coarse-grained model with two length scales. The main objective of the study is to investigate the existence and relative stability of the 3D icosahedral quasicrystals. Specifically, the ratio of the two length scales is chosen as the golden ratio, thus favouring the formation of icosahedral quasicrystals. Besides the 3D icosahedral quasicrystals, a number of possible 2D quasicrystals and periodic crystal structures are included as candidate phases in the study. A comparison of the free energies of the different candidate phases is used to construct the phase diagram of the model system. The theoretical study predicts that the 3D icosahedral quasicrystals are stable phase within the model systems.

2. Model and method

2.1. Theoretical model

The structure of a system exhibiting ordered phases can be described by its density distribution or density profile $\varphi(\mathbf{r})$. The thermodynamic behaviour of the system can be determined by a free energy functional $F[\varphi(\mathbf{r})]$. In particular, the equilibrium phases of the system are determined by minimizing the free energy functional with respect to the density profile. In the present study, a generic coarse-grained free energy functional is used,

$$F[\varphi(\mathbf{r})] = \frac{1}{V}\int\int \frac{\gamma}{2}[\varphi(\mathbf{r})G(\mathbf{r},\mathbf{r}')\varphi(\mathbf{r}')]\mathrm{d}\mathbf{r}\mathrm{d}\mathbf{r}' + \frac{1}{V}\int\left[-\frac{\varepsilon}{2}\varphi^2(\mathbf{r}) - \frac{\alpha}{3}\varphi^3(\mathbf{r}) + \frac{1}{4}\varphi^4(\mathbf{r})\right]\mathrm{d}\mathbf{r}, \quad (1)$$

where γ, ε and α are phenomenological parameters of the system and the function $G(\mathbf{r},\mathbf{r}') = G(|\mathbf{r}-\mathbf{r}'|)$ is a two-body correlation potential. In this expression, the polynomial term corresponds to the bulk free energy of the system, whereas the term involving $G(\mathbf{r},\mathbf{r}')$ describes the free energy cost of inhomogeneity of the system. In particular, different choices of $G(\mathbf{r},\mathbf{r}')$ result in the selection of different dominant modes at particular length scales, thus promoting the formation of ordered structures. When one length scale is selected by $G(\mathbf{r},\mathbf{r}')$, simple crystal structures with one length-scale, such as the body-centred-cubic (BCC) phase, are stabilized [18, 37]. When the function $G(\mathbf{r},\mathbf{r}')$ is chosen such that two length scales with proper length ratios are selected, complex ordered phases including quasicrystals can be stabilized [20, 21, 27, 38, 39].

The selection of two length scales in the potential $G(\mathbf{r},\mathbf{r}')$ can be realized by introducing gradient terms [20, 21, 27, 29], such that the wave vectors of the basic modes of density fluctuations are located on two spherical shells with radii determined by the two length scales. A more general method to introduce two or more length scales is using an effective function such that it has two equal-depth minima. This selection of two length scales can be realized by a steplike function [24] or a Gaussian-type potential family [25, 26]. In previous studies, most of these models aimed at the study of 2D systems in order to understand the formation and stability of soft quasicrystals.

In the present study, we examine the occurrence and stability of 3D icosahedral quasicrystals within the above theoretical framework of equation (1) with an interaction potential possessing two length scales. Specifically, we adopt the Gaussian-polynomial function proposed by Barkan *et al* [26] to describe the pair interaction potential,

$$G(r) = \mathrm{e}^{-\sigma^2 r^2/2}(c_0 + c_2 r^2 + c_4 r^4 + c_6 r^6 + c_8 r^8), \quad (2)$$

where σ and c_i are model parameters. The corresponding pair interaction potential in the Fourier space is

$$\hat{G}(k) = \mathrm{e}^{-k^2/2\sigma^2}(d_0 + d_2 k^2 + d_4 k^4 + d_6 k^6 + d_8 k^8), \quad (3)$$

where the coefficients d_i are related to c_i as,

Table 1. Potential parameters used in the present study.

σ	d_0	d_2	d_4	d_6	d_8
0.568 81	1.969 17	−14.949 76	37.445 44	−38.839 19	13.999 17
	c_0	c_2	c_4	c_6	c_8
	1.0	−0.826 761	0.131 652	−0.006 271	0.000 087

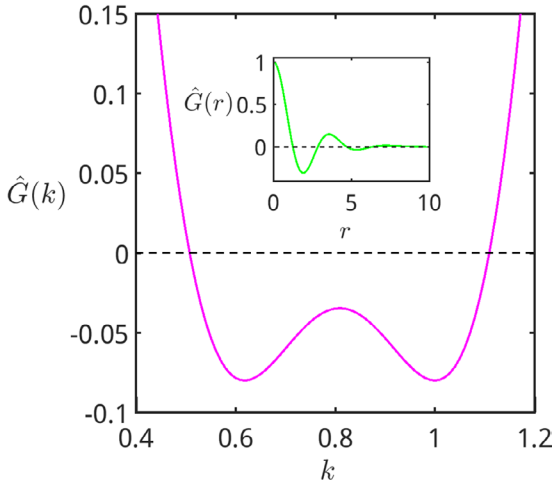

Figure 1. One-dimensional schematic plot of the pair interaction potential in the model (1) used in the present study. $\hat{G}(k)$ is the Fourier transform whose first minimum is at $k = 1/(2\cos(\pi/5))$, and the second one is at $k = 1$. The inset is the corresponding $G(r)$ in the real space.

$$c_{2i} = \frac{1}{2\pi}\sum_{j=1}^{4}(-1)^j \frac{2^{j-i}}{(j-i)!}\left(\frac{j!}{i!}\right)^2 d_{2j}\sigma^{2(i+j+1)}. \quad (4)$$

The parameters of the model are chosen such that the interaction potential $\hat{G}(k)$ has two equal-depth minima at $|\mathbf{k}| = 1$ and $|\mathbf{k}| = q$. To highlight the formation of icosahedral quasicrystals, the second characteristic length scale is chosen as $q = 1/(2\cos(\pi/5))$. Specifically, the model parameters are determined by solving the following five equations,

$$\begin{aligned} G(0) = c_0 &= \frac{1}{2\pi}\sum_{j=0}^{4} 2^j j!\, d_{2j}\sigma^{2(j+1)} = 1, \\ \hat{G}(1) &= \hat{G}(q) = \hat{G}_{\min} := -0.08, \\ \left.\frac{\mathrm{d}\hat{G}}{\mathrm{d}k}\right|_{k=1} &= \left.\frac{\mathrm{d}\hat{G}}{\mathrm{d}k}\right|_{k=q} = 0. \end{aligned} \quad (5)$$

Furthermore the choice of the parameter σ does not affect the above required feature of potential function. The specific coefficients used in our study are summarized in table 1. The corresponding pair potential function is plotted in figure 1.

The parameter γ in equation (1) describes the strength of the pair interaction potential. In what follows, we will investigate the formation and stability of quasicrystals and crystals when γ is either finite or infinite. At the limit of $\gamma \to \infty$, all the Fourier modes of φ should be restricted to be on the spherical surfaces in 3D cases and the circles in 2D ones in the Fourier space with radii $|\mathbf{k}| = 1$ and $|\mathbf{k}| = q$. In this case, the interaction potential term becomes zero, and only the bulk

free energy shall be analyzed. When γ is finite, the free energy functional of equation (1) can be recast in a scaled form by defining new parameters, $F = \gamma^2\tilde{F}$, $\varphi = \sqrt{\gamma}\phi$, $\varepsilon = \gamma\tilde{\varepsilon}$ and $\alpha = \sqrt{\gamma}\tilde{\alpha}$. With the scaled parameters, the coarse-grained free energy model (1) becomes,

$$\tilde{F}[\phi(\mathbf{r})] = \frac{1}{V}\int\int\frac{1}{2}[\phi(\mathbf{r})G(\mathbf{r},\mathbf{r}')\phi(\mathbf{r}')]\mathrm{d}\mathbf{r}\mathrm{d}\mathbf{r}' + \frac{1}{V}\int\left[-\frac{\tilde{\varepsilon}}{2}\phi^2(\mathbf{r}) - \frac{\tilde{\alpha}}{3}\phi^3(\mathbf{r}) + \frac{1}{4}\phi^4(\mathbf{r})\right]\mathrm{d}\mathbf{r} \quad (6)$$

Therefore for all finite values of γ ($\gamma \neq 0$), the phase behaviour of our model (6) is governed by the scaled parameters $\tilde{\varepsilon} = \varepsilon/\gamma$ and $\tilde{\alpha} = \alpha/\sqrt{\gamma}$.

2.2. Numerical methods

The possible equilibrium phases of the system correspond to local minima of the free energy functional. Specifically the candidate phases are obtained as solutions of the Euler–Lagrange equation of the free energy functional,

$$\frac{\delta F}{\delta\phi(\mathbf{r})} = 0. \quad (7)$$

The Euler–Lagrange equation (7) is a nonlinear partial differential equation. For structures with quasicrystalline order, an efficient method is the projection method formulated in the Fourier space [35]. The projection method is based on the fact that a d-dimensional quasicrystal is a combination of a class of exponentials $\{e^{i\mathbf{k}^T\mathbf{r}}\}$, $\mathbf{r}\in\mathbb{R}^d$, $\mathbf{k}$, located on a d-dimensional quasilattice. The expansion coefficients are related to the diffraction intensities which can be calculated in an n-dimensional ($n \geqslant d$) periodic region. In other words, the Fourier spectrum of the quasiperiodic structure can be lifted into an n-dimensional periodic structures. Specifically, the n-dimensional reciprocal vectors can be spanned by a set of bases $\mathbf{b}_i$, which are the primitive reciprocal vectors in the n-dimensional reciprocal space, with integer coefficients. That is, an n-dimensional reciprocal vector can be written as $\mathbf{H} = \mathbf{B}\mathbf{h}$, where $\mathbf{h}\in\mathbb{Z}^n$ and $\mathbf{B} = (\mathbf{b}_1, \ldots, \mathbf{b}_n) \in \mathbb{R}^{n\times n}$ is the reciprocal primitive lattice. The physical, d-dimensional, wavevector $\mathbf{k}$ is then obtained from the n-dimensional vector $\mathbf{H}$ by a projection, $\mathbf{k} = P\mathbf{H}$, where P is a projection matrix of $d\times n$-order. The dimensionality n and the specific form of the projection matrix is determined by the structure of the ordered phases. The expression of P is not unique and relies on the symmetry of the quasicrystals. The projection matrices could be analysed by the group theory and the representation theory [14, 40]. From the view of numerical computation, it can be easily determined by the choice of the basis vectors [35].

Using the n-dimensional periodic lattice and the projection matrix, the expansion of any d-dimensional quasiperiodic function $\phi(\mathbf{r})$ can be written in the form,

$$\phi(\mathbf{r}) = \sum_{\mathbf{h}\in\mathbb{Z}^n}\hat{\phi}(\mathbf{h})e^{i[P\mathbf{B}\mathbf{h}]^T\cdot\mathbf{r}}, \quad \mathbf{r}\in\mathbb{R}^d, \quad (8)$$

where the Fourier coefficients $\hat{\phi}(\mathbf{h})$ are calculated by the n-dimensional L^2-inner product, $\hat{\phi}(\mathbf{h}) = \langle\tilde{\phi}(\tilde{\mathbf{r}}), e^{-i(\mathbf{B}\mathbf{h})^T\tilde{\mathbf{r}}}\rangle$, with $\tilde{\mathbf{r}} = \sum_{i=1}^n s_i\mathbf{a}_i \in \mathbb{R}^n$, $0 \leqslant s_i \leqslant 1$. Here $\mathbf{a}_i$, $i = 1, 2, .., n$, are the primitive lattice vectors forming the primitive lattice A of the n-dimensional periodic structure. The primitive vectors satisfy the dual relationship, $\mathbf{a}_i\cdot\mathbf{b}_j = 2\pi\delta_{ij}$. Furthermore, the function $\tilde{\phi}(\tilde{\mathbf{r}})$ is the n-dimensional inverse Fourier transform of $\hat{\phi}(\mathbf{h})$. One simple observation is that the expansion of equation (8) allows us to treat the d-dimensional quasiperiodic structure as a slice of an n-dimensional periodic structure whose orientation is determined by P. For description of the position of the quasilattice in d-dimensional Fourier space, we use $\mathbf{k}$ instead of $P\mathbf{B}\mathbf{h}$ in equation (9). With this notation, the projection method has the following form,

$$\phi(\mathbf{r}) = \sum_{\mathbf{h}\in\mathbb{Z}^n}\hat{\phi}(\mathbf{h})e^{i\mathbf{k}^T\mathbf{r}}, \quad (9)$$

where $\mathbf{k} = \sum_{i=1}^n h_i(P\mathbf{b}_i) \in \mathbb{R}^d$. Despite the similarity with the common Fourier transform, it is important to note that the distribution of $\mathbf{k}$ is not a periodic lattice. Rather, it is a quasilattice generated from a high-dimensional periodic lattice by the projection matrix P.

The free energy functional in terms of the Fourier coefficients $\hat{\phi}(\mathbf{h})$ can be obtained by expanding the order parameter $\phi(\mathbf{r})$ in the form of equation (9) and inserting it into equation (1). For a given structure of interest, the reciprocal lattice vectors are determined by its symmetry, and the optimal Fourier coefficients are obtained by minimizing the free energy functional. In our previous work [35], it has been shown that, when using the projection method, it suffices to have a free energy functional defined in the lower (physical) d-dimensional space. Therefore the computations are implemented in the n-dimensional periodic unit cell, while the final results represent the d-dimensional structures through equation (9). As a special case of quasiperiodic structures, a d-dimensional periodic structure can be described within the projection method by setting the projection matrix as a $d\times d$ identity matrix. In this case the projection method is reduced to the commonly used Fourier-spectral method. This does not provide any computational advantage when it comes to periodic crystals. However, this formulation provides a unified computational framework for studying the crystals and quasicrystals.

In practice, we use a relaxation method to obtain solutions of the Euler–Lagrange equation of the free energy functional. Inserting the generalized Fourier expansion (9) into equation (1), the free energy functional becomes a function of the Fourier coefficients,

$$F = \frac{\gamma}{2}\sum_{\mathbf{h}}|\hat{\phi}(\mathbf{h})|^2\hat{G}(\mathbf{h}) - \frac{\varepsilon}{2}\sum_{\mathbf{h}_1+\mathbf{h}_2=0}\hat{\phi}(\mathbf{h}_1)\hat{\phi}(\mathbf{h}_2) - \frac{\alpha}{3}\sum_{\mathbf{h}_1+\mathbf{h}_2+\mathbf{h}_3=0}\hat{\phi}(\mathbf{h}_1)\hat{\phi}(\mathbf{h}_2)\hat{\phi}(\mathbf{h}_3) + \frac{1}{4}\sum_{\mathbf{h}_1+\mathbf{h}_2+\mathbf{h}_3+\mathbf{h}_4=0}\hat{\phi}(\mathbf{h}_1)\hat{\phi}(\mathbf{h}_2)\hat{\phi}(\mathbf{h}_3)\hat{\phi}(\mathbf{h}_4). \quad (10)$$

Instead of solving the nonlinear Euler-Lagrange equation directly, we adopt an iterative method to solve the

optimization problem. Specifically, the Fourier coefficients are iterated according to the Allen–Cahn dynamic equation,

$$\frac{\partial\hat{\phi}(\mathbf{h})}{\partial t} = -\frac{\partial F}{\partial\hat{\phi}(\mathbf{h})} = \varepsilon\hat{\phi}(\mathbf{h}) + \alpha\hat{\phi}^2(\mathbf{h}) - \hat{\phi}^3(\mathbf{h}) - \gamma\hat{G}(\mathbf{h})\phi(\mathbf{h}). \quad (11)$$

It should be pointed out that the variable t is a parameter controlling the iteration steps, and it does not correspond to real time. In this expression the quadratic and cubic terms are given by,

$$\hat{\phi}^2(\mathbf{h}) = \sum_{\mathbf{h}_1+\mathbf{h}_2=\mathbf{h}} \hat{\phi}(\mathbf{h}_1)\hat{\phi}(\mathbf{h}_2),$$
$$\hat{\phi}^3(\mathbf{h}) = \sum_{\mathbf{h}_1+\mathbf{h}_2+\mathbf{h}_3=\mathbf{h}} \hat{\phi}(\mathbf{h}_1)\hat{\phi}(\mathbf{h}_2)\hat{\phi}(\mathbf{h}_3). \quad (12)$$

From these expressions it is obvious that the nonlinear (quadratic and cubic) terms in equation (11) are n-dimensional convolutions in the reciprocal space. A direct evaluation of these nonlinear terms will be computationally expensive. Instead, these terms are simple dot-multiplication in the n-dimensional real space and the computation of these nonlinear terms in the real space is straightforward. The pseudospectral method takes advantage of this observation by evaluating the convolutions in the Fourier space and the nonlinear terms in the real space, thus providing an efficient technique to find solutions of the Euler–Lagrange equation. The pseudospectral method requires access to the density function in the real and reciprocal spaces. The transformation between the real-space and reciprocal space was done by performing fast Fourier transformation (FFT) in the n-dimensional space.

An accelerated algorithm, corresponding to a hybrid of the semi-implicit scheme and the Nesterov gradient method [41], is used to update the above dynamic equation (11). For a set of given initial values $\hat{\phi}^0(\mathbf{h})$, the first step of this scheme is to set, $\hat{\psi}^0(\mathbf{h}) = \hat{\phi}^0(\mathbf{h})$. Then the $(n+1)$th ordered parameter $\hat{\phi}^{n+1}(\mathbf{h})$ is updated according to

$$\hat{\phi}^{n+1}(\mathbf{h}) + \gamma\Delta t\,[\hat{G}(\mathbf{h})\hat{\phi}^{n+1}(\mathbf{h})] = \hat{\psi}^n(\mathbf{h}) + \Delta t\cdot u(\hat{\psi}^n(\mathbf{h})),$$
$$\hat{\psi}^{n+1}(\mathbf{h}) = (1-\beta)\hat{\phi}^{n+1}(\mathbf{h}) + \beta\hat{\phi}^n(\mathbf{h})), \quad (13)$$

where Δt is the time step length, $u(\hat{\psi}(\mathbf{h})) = \varepsilon\hat{\psi}(\mathbf{h}) + \alpha\hat{\psi}^2(\mathbf{h}) - \hat{\psi}^3(\mathbf{h})$ and $0 < \beta < 1$. When $\beta = 0$, the above scheme becomes the semi-implicit method.

Starting from an initial configuration with a specified symmetry, a steady state solution of equation (11), corresponding to a local minimum of the free energy functional, is obtained. Using initial configurations with different symmetries leads to different ordered structures as solutions of the optimization problem. The ordered structures corresponding to these solutions are taken as candidate phases of the problem. The free energies of these candidate structures are then compared and used to construct phase diagrams of the system.

3. Results and discussion

Using the projection method outline above, we obtained a number of possible ordered phases for the model system. Their relative stability is then examined by comparing their free energy. In what follows we will focus on the occurrence and stability of the 3D icosahedral quasicrystals and related ordered structures, thus we will set the ratio between the two characteristic length scales in the interaction potential G to $q = 1/(2\cos(\pi/5))$. It is possible that the 2D decagonal quasicrystals are the equilibrium phases of this model system. In the projection method, the 3D icosahedral quasicrystals can be obtained from a projection of periodic structures in 6-dimensional space, while the decagonal quasicrystals can be embedded into 4-dimensional periodic structures. Furthermore, various periodic structures, corresponding to crystals with 2-fold, 6-fold and BCC symmetries, are included as candidate phases in our study. On the other hand, other quasicrystals, such as the 2D dodecagonal and octagonal quasicrystals, which occur with different characteristic length scales [26, 28], are not included in the current study. In practice, the n-dimensional Fourier space is discretized using 16 basis functions along each direction. The total number of variables is thus 16^n. We remark that the projection method works equally well if different numbers of basis functions along each dimension are used.

The accelerated method described above is used to solve equation (11). It is observed that the accelerated algorithm converges 5–7 times faster than the semi-implicit scheme in order to achieve at the error of $\max_{\mathbf{h}}|(\delta F/\delta\phi)(\mathbf{h})|$ less than 10^{-6}. This accelerated scheme allows us to investigate the stability of 3D icosahedral quasicrystals efficiently. For the cases of periodic crystals and quasicrystals, the computation starts with initial configurations with the desired symmetries. The choice of the initial configurations is another factor which could be used to speed up the computations by reducing the number of iterations. If the initial symmetric structure is a local minimum of the free energy functional for a given set of model parameters, the calculation will lead to a converged solution with the prescribed symmetry. In the case that the chosen symmetry of the initial configuration does not correspond to a local minimum, the iteration procedure will lead to other phases, or more commonly, to the trivial solution $\phi(\mathbf{r}) = 0$ corresponding to the homogeneous phase. It should be noted that the homogeneous phase is always a solution of the Euler–Lagrange equation.

3.1. Candidate patterns

The free energy functional of equation (1) can be used to explore the formation and stability of ordered structures. Structures with icosahedral symmetry are obtained by setting the ratio of the two characteristic length scale to $q = 1/(2\cos(\pi/5))$ in the interaction potential function. The icosahedral quasicrystals can be embedded into 6-dimensional periodic structures. Therefore, for obtaining numerical solutions of the 3D icosahedral quasicrystals, the computation

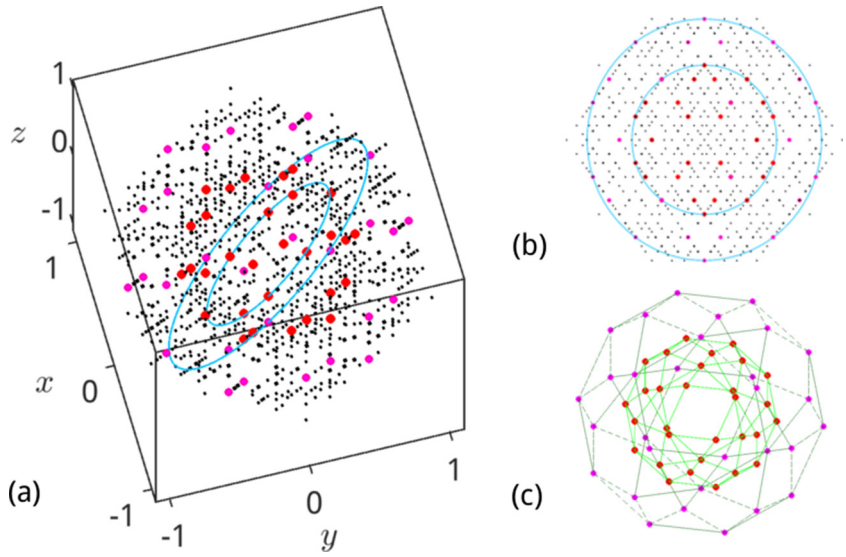

Figure 2. Diffraction of 3D icosahedral quasicrystal computed by the projection method. Only these Fourier modes whose diffraction intensity is larger than 1×10^{-4} are shown. The red and magenta points represent the basic 60 Fourier modes. The red points represent the largest 30 diffraction points located on the spherical surface of radius $q = 1/(2\cos(\pi/5))$, while the rest of 30 magenta points located on the spherical surface of radius 1. (a) 3D diffraction image. (b) Diffraction pattern taken in a plane normal to the vector $(1/q, -1, 0)$, in the Fourier space. The spherical surfaces of radii 1 and q are indicated. The 10-fold rotation symmetry of the diffraction pattern is indicated by the 10 peaks observed on each spherical surface. (c) Geometric figure, made by connecting the ends of 30 basic modes on each spherical surface, respectively, is two icosidodecahedra, with 20 triangular faces and 12 pentagonal faces. Edges on spherical surfaces with radii 1 and q are indicated with black and green lines.

is carried out in the 6-dimensional primitive reciprocal lattice $B = [0,\ 1]^6$ correspondingly the primitive hypercube $A = [0, 2\pi]^6$. After evolving the dynamical equation (11), we can obtain the optimized Fourier coefficients $\hat{\phi}(\mathbf{h})$ which correspond to the solution of Euler–Lagrange equation (7). Then using the projection method, we can reconstruct the 3D quasicrytalline pattern by a 3×6-order projection matrix P,

$$P = \begin{pmatrix} 1 & \tau/2 & \tau/2 & \tau/2 & 0 & 0 \\ 0 & 1/2 & -1/2 & -1/2 & 1 & 0 \\ 0 & (1-\tau)/2 & (\tau-1)/2 & (1-\tau)/2 & 0 & 1 \end{pmatrix}, \quad (14)$$

where $\tau = 2\cos(\pi/5)$ is the golden ratio. With the two length scale in the golden ratio, an alternative mechanism for reinforcing icosahedral symmetry is possible by the triangular interactions. Applying the projection method and the accelerated scheme to the dynamical equation (11), the 3D icosahedral quasicrytalline structure has been obtained. As an example of the converged solutions, the diffraction pattern of a 3D icosahedral phase is given in figure 2.

When the ratio of the two length scales is set at $q = 1/(2\cos(\pi/5))$, the system tends to form 2D 10-fold symmetric quasicrystals. Since the decagonal quasicrystal can be realize as the projection from a 4D periodic structure, we carried out the computation in the 4D primitive reciprocal lattice $B = [0,\ 1]^4$, correspondingly the primitive hypercube $A = [0, 2\pi]^4$. After obtaining the optimized Fourier coefficients $\hat{\phi}(\mathbf{h})$ by the relaxation equation (11), we can project the solution onto 2D space by the projection matrix P,

$$P = q\begin{pmatrix} 1 & \cos(\pi/5) & \cos(2\pi/5) & \cos(3\pi/5) \\ 0 & \sin(\pi/5) & \sin(2\pi/5) & \sin(3\pi/5) \end{pmatrix}. \quad (15)$$

The diffraction pattern contains 20 basic Fourier modes, with 10 vectors located on the circle of $|\mathbf{k}| = q$, and the other ten on the circle of $|\mathbf{k}| = 1$. The ten wavevectors satisfy the decagonal symmetry on each circle. The distribution of ϕ in the real space and the diffraction pattern in the Fourier space are similar to what in the [28].

It should be noted that quasicrystals are the space-filling structures without spatial periodicity. As such, computations on quasicrystals using finite domains will lead to inaccurate results. On the other hand, quasicrystals can be embedded into the higher-dimensional periodic structures. For periodic structures, regardless of dimensions, their studies can be reduced to a primitive domain which may be a hyper-cube, or, more generally, a hyper-parallelepiped. The proposed projection method has the capability of adaptively optimizing computational domain, with respect to the lengths and angles, even in higher-dimensional space [27]. In the present work, we use hyper-cubes in our study of the 3D icosahedral and 2D decagonal quasicrystals. It is noted that the choice of the high-dimensional lattice is not unique. The hyper-cubes are the simplest lattices which can be used to construct quasicrystals.

The projection method can be used to obtain periodic structures as local minima of the free energy functional of equation (1) by setting the projection matrix as an identity matrix. Due to the existence of two characteristic length scales in the model of equation (1), two stable periodic structures with the same symmetry but different lattice spacings can be obtained [25, 28, 29, 42]. These structures are termed as *sibling periodic crystals*. When $q \neq 1$, a number of periodic phases with their sibling periodic crystals, including 2D 2-, and 6-fold symmetric patterns and a 3D BCC spherical phase (with space group $Im\bar{3}m$), have been obtained from our

calculations. The basic Fourier vectors of two sibling periodic phases are located at the spherical surfaces or circles with radii $|\mathbf{k}| = 1$ and $|\mathbf{k}| = q$, respectively.

3.2. Phase behaviour at the limit $\gamma \to +\infty$

At the limit $\gamma \to \infty$, the wave vectors of the density profiles of the free energy functional of equation (1) are restricted to the basic Fourier modes whose magnitude is either $|\mathbf{k}| = 1$ or $|\mathbf{k}| = q$, lying on two spherical shells in the Fourier space. In this case the interaction potential term becomes zero, otherwise, the free energy value will increase indefinitely. Therefore it is only required to analyze the bulk free energy part. After performing a rescaling of the order parameter $\varphi \to \alpha\varphi$, the free energy functional of the system can be written in the scaled form,

$$\begin{aligned}\alpha^{-4}F = &-\frac{1}{2}\varepsilon^* \sum_{|\mathbf{k}|=1,q} \hat{\varphi}(\mathbf{h})\hat{\varphi}(-\mathbf{h}) \\ &-\frac{1}{3}\sum_{|\mathbf{k}_i|=1,q} \hat{\varphi}(\mathbf{h}_1)\hat{\varphi}(\mathbf{h}_2)\hat{\varphi}(-\mathbf{h}_1-\mathbf{h}_2) \\ &+\frac{1}{4}\sum_{|\mathbf{k}|=1,q} \hat{\varphi}(\mathbf{h}_1)\hat{\varphi}(\mathbf{h}_2)\hat{\varphi}(\mathbf{h}_3)\hat{\varphi}(-\mathbf{h}_1-\mathbf{h}_2-\mathbf{h}_3), \qquad (16)\end{aligned}$$

where $\varepsilon^* = \varepsilon/\alpha^2$. The phase behaviour of this free energy functional can be analyzed using the basic modes approximation (BMA) [43]. For a given candidate structure, the wavevectors $\mathbf{k}$ should satisfy corresponding symmetries. The set of Fourier coefficients $\hat{\varphi}(\mathbf{h})$, which gives rise to the lowest values of F for a given parameters ε^*, determines the stable phases of the free energy function (16). The 60 basic modes of the 3D icosahedral quasicrystal have the icosahedral symmetry, as shown in figure 2(c). The corresponding free energy function (16) becomes,

$$\begin{aligned}\alpha^{-4}\ F_{3D} = &-\varepsilon^*[15\hat{\varphi}_1^2 + 15\hat{\varphi}_q^2] - [40\hat{\varphi}_1^3 + 120\hat{\varphi}_1^2\hat{\varphi}_q \\ &+ 120\hat{\varphi}_1\hat{\varphi}_q^2 + 40\hat{\varphi}_q^3] \\ &+\left[\frac{1665}{2}\hat{\varphi}_1^4 + 1440\hat{\varphi}_1^3\hat{\varphi}_q + 3150\hat{\varphi}_1^2\hat{\varphi}_q^2 + 1440\hat{\varphi}_1\hat{\varphi}_q^3\right. \\ &\left.+ \frac{1665}{2}\hat{\varphi}_q^4\right], \qquad (17)\end{aligned}$$

where $\hat{\varphi}_1$ and $\hat{\varphi}_q$ are the Fourier coefficients on the spherical surfaces of $|\mathbf{k}| = 1$ and $|\mathbf{k}| = q$, respectively. For the 2D decagonal quasicrystals, there are twenty Fourier modes with ten vectors located on the circle of $|\mathbf{k}| = 1$, and the other ten on the circle of $|\mathbf{k}| = q$ [28]. These Fourier modes of the decagonal quasicrystal located on two circles are collinear. When $\gamma \to \infty$, the free energy function of equation (16) of the 2D 10-fold symmetric quasicrystal is given by,

$$\begin{aligned}\alpha^{-4}F_{10} = &-5\varepsilon^*[\hat{\varphi}_1^2 + \hat{\varphi}_q^2] - 20[\hat{\varphi}_1^2\hat{\varphi}_q + \hat{\varphi}_1\hat{\varphi}_q^2] \\ &+\frac{15}{2}[9\hat{\varphi}_1^4 + 8\hat{\varphi}_1^3\hat{\varphi}_q + 28\hat{\varphi}_1^2\hat{\varphi}_q^2 + 8\hat{\varphi}_1\hat{\varphi}_q^3 + 9\hat{\varphi}_q^4], \\ &\qquad (18)\end{aligned}$$

where $\hat{\varphi}_1$ and $\hat{\varphi}_q$ are the Fourier coefficients on the circles of $|\mathbf{k}| = 1$ and $\mathbf{k} = q$, respectively. The minima of equation (17)

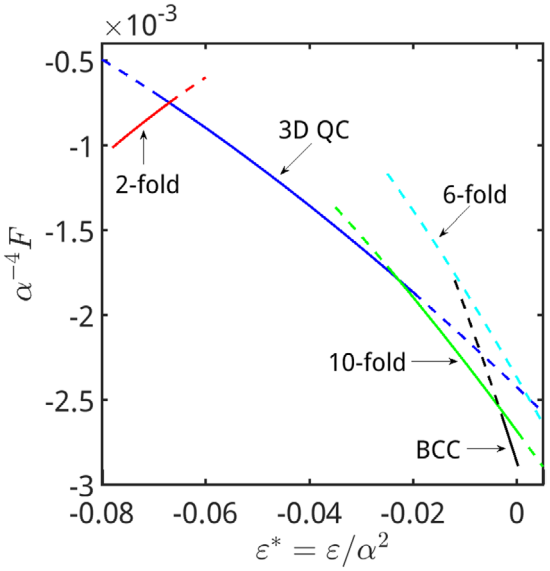

Figure 3. The free energy values of (16) with respect to parameter ε^*. Lines track the free energy $\alpha^{-4}F$ of the labeled structures, solid where these are locally stable, dashed where they are locally metastable.

and equation (18) can be obtained by numerical optimization methods, such as the steepest descent method. For periodic crystals of 2-, and 6-fold symmetric structures and the 3D BCC spherical phase, we can directly obtain the minimum values F^* of the free energy (16),

$$\begin{aligned}\alpha^{-4}F_2^* &= \frac{1}{6}\varepsilon^*, \\ \alpha^{-4}F_6^* &= -\frac{4}{15^3}(1+\sqrt{1+15\varepsilon^*}) \\ &\quad -\frac{2}{15^2}(3+2\sqrt{1+15\varepsilon^*})\varepsilon^* - \frac{1}{10}\varepsilon^{*2}, \\ \alpha^{-4}F_{\mathrm{BCC}}^* &= v^2(-12\varepsilon^* - 16v + 135v^2), \qquad (19)\end{aligned}$$

where $v = (2+\sqrt{4+90\varepsilon^*})/45$. The free energy of the different candidate structures as a function of ε^* is plotted in figure 3. The phase boundaries of the different phase transitions can be determined from the free energy comparison. For $\varepsilon^* \leqslant -0.067$, the 2-fold symmetric pattern has the lowest free energy. For $-0.067 \leqslant \varepsilon^* \leqslant -0.029$, the 3D icosahedral quasicrystal is the most stable. For $-0.029 \leqslant \varepsilon^* \leqslant -0.0035$, the 2D 10-fold symmetric quasicrystal is the most energetically favourable. For $\varepsilon^* \geqslant -0.0035$, the 3D BCC spherical phase becomes stable. The 2D 6-fold symmetric structure is a metastable in this parameter region. The phase behaviour of the model system at the limit $\gamma \to \infty$ is summarized in the phase diagram in the $\varepsilon - \alpha$ space (figure 4).

3.3. Phase behaviour for finite γ

In this subsection, we will use the projection method to investigate the phase behaviour of the model system (1) for finite γ. As mentioned in section 2.1, for all finite values of γ ($\gamma \neq 0$), we can study the scaled model of equation (6). In this case, more non-zero Fourier modes arise besides those on

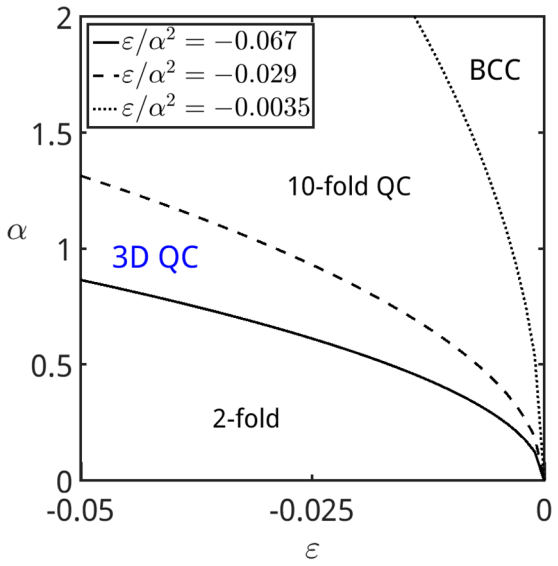

Figure 4. Phase diagram obtained by the BMA method of the model equation (16) for $q = 1/(2\cos(\pi/5))$ and $\gamma \to \infty$. The phase boundaries are lines of constant $\varepsilon^* = \varepsilon/\alpha^2$.

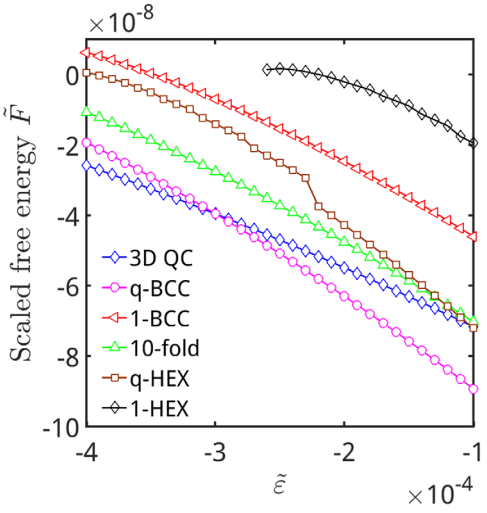

Figure 5. The free energies of various structures as functions of $\tilde{\varepsilon}$ on the phase path of fixed $\tilde{\alpha} = 0.08$.

the spherical shells with radii $|\mathbf{k}| = 1$ and $|\mathbf{k}| = q$. The candidate structures for the construction of phase diagram include the 3D icosahedral quasicrystal, 2D decagonal quasicrystal, as well as periodic crystals of BCC, 2-, and 6-fold (HEX) symmetric phases. Due to the existence of two characteristic length scales in the model equation (6), the periodic structures with the same symmetry but different lattice spacings can be obtained from our calculations. The basic Fourier vectors of two sibling periodic phases are located at the spherical shells with radii $|\mathbf{k}| = 1$ or $|\mathbf{k}| = q$. Therefore, there are 8 candidate ordered structures considered in our calculations.

We start with the phase behaviour of the model system as a function of the parameter $\tilde{\varepsilon}$ for fixed $\tilde{\alpha} = 0.08$. The free energy difference of the candidate patterns, including 3D icosahedral quasicrystal, 10-fold symmetric quasicrystal, and q-BCC, 1-BCC, q-HEX, 1-HEX, phases as function of $\tilde{\varepsilon}$ is presented in figure 5. Here q-BCC denotes the periodic crystal BCC whose basic Fourier vectors are located at the spherical surface with radius $|\mathbf{k}| = q$. The notations of 1-BCC, q-HEX and 1-HEX have the similar meanings. The free energy plot of the 2-fold symmetric pattern is not given in this figure since this structure becomes unstable in this parameter region. From the results shown in figure 5, it is obvious that only the 3D quasicrstal and the q-HEX phase have global stable regions with the lowest free energy, whereas the other four candidate structures have relative higher free energies. As $\tilde{\varepsilon}$ is increased, the phase transition sequence is from 3D QC to q-BCC with the phase transition occurs at $\tilde{\varepsilon} = 3 \times 10^{-4}$.

In order to analyze the contributions to the free energy from the different Fourier modes, it is informative to separate the Fourier modes into two parts: basic modes and higher-harmonics. The basic modes are those modes with nonzero coefficients lying on the spherical shells with radii 1 and $q = 1/(2\cos(\pi/5))$, and the higher-harmonics are other Fourier modes with nonzero coefficients. The basic part of the free energy is defined by the contribution of the basic Fourier modes to the free energy, while the higher-harmonic part of energy is the remainder when subtracting the basic part of energy from the total energy. The basic part of energy can be calculated analytically using the BMA method. The analytic expressions of the basic part of energy for quasicrystals are given in the section 3.2, while for periodic crystals, shown in the [28]. Figure 6 gives the basic and higher-harmonic contributions to the free energy for the 3D QC, 10-fold, q-BCC and 1-BCC structures. The separated energies for the metastable phases of q-HEX and 1-HEX are not given in this figure. From figure 6(a), it can be concluded that the quasicrystals, including the 3D QC and 2D 10-fold symmetric quasicrystal, are favoured by the basic modes. Since they have the larger number of nonzero Fourier modes, 60 and 20, respectively, located on the spherical surfaces or circles with radii of 1 and q, rather than that of periodic crystals whose basic modes lie on one of the two spherical surfaces or circles. Therefore the non-zero basic models of quasicrystals can form more resonant triplets of modes in the Fourier space that can reduce the free energy to a larger degree. Specifically, 960 and 120 triangles are formed for 3D QC and 2D 10-fold symmetric quasicrystal, respectively. On the other hand, since the energy penalty factor γ is finite, the higher-harmonics cannot be completely ignored. Meanwhile, the interaction terms are no longer zero, which increases the energy. As figure 6(b) shows, these higher-harmonics have significant impacts on the free energy of the system. The q-BCC phase has the lowest higher-harmonics contribution to the free energy, since its Fourier modes with nonzero coefficients have smaller fourth-order terms than quasicrystals. It can be observed that the quadratic and the quartic power terms increase the free energy. Due to the competition of the basic modes and higher-harmonics, the stable phases are 3D QC and q-BCC patterns as α increases, whereas the decagonal quasicrystals become metastable.

The phase transition sequence for other values of $\tilde{\alpha}$ can be obtained by repeating the free energy comparison among the candidate structures. The results of the phase

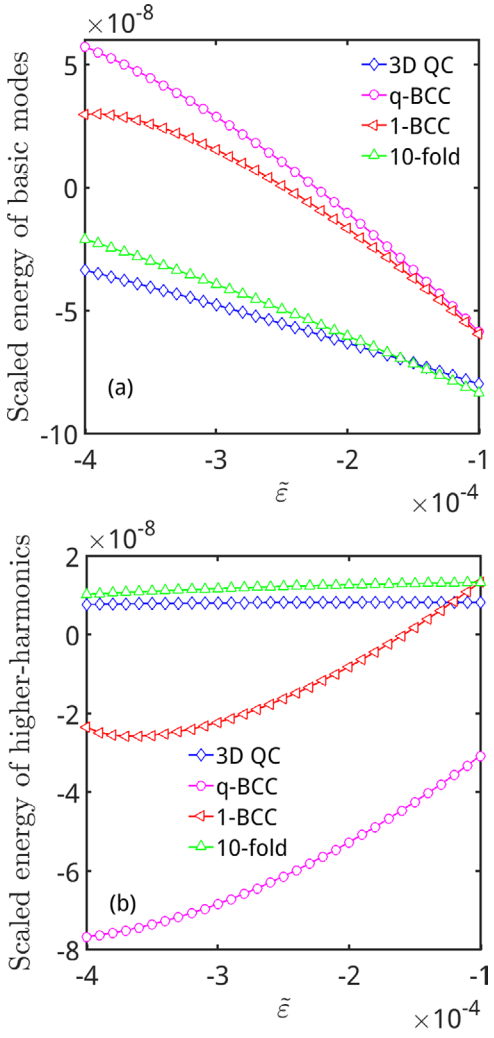

Figure 6. (a) Basic modes energy and (b) higher-harmonic energy of various patterns as functions of $\tilde{\varepsilon}$ for fixed $\tilde{\alpha} = 0.08$.

transition sequences can be summarized in terms of phase diagrams in the $\tilde{\varepsilon}$-$\tilde{\alpha}$ plane. The phase diagram in the range of $-5 \times 10^{-4} \leqslant \tilde{\varepsilon} \leqslant -1.7 \times 10^{-4}$ and $0.04 \leqslant \tilde{\alpha} \leqslant 0.11$ is presented in figure 7 for our model system. Besides the 3D QC and q-BCC structures discussed above, the homogeneous phase (disordered) is included in the phase diagram. The regions of stability of the different phases are obtained by comparing the free energy of these candidate structures. Since the contribution from the higher-harmonics becomes significant for the cases of finite γ, the numerical phase diagram demonstrates a different phase behaviour compared with the approximated phase diagram at $\gamma \to +\infty$ obtained by the BMA method. The 2-fold symmetric structures, which are stable in the phase diagram of $\gamma \to \infty$, disappear in these parameter region. Meanwhile, the 2D decagonal quasicrystals become metastable in the range of parameters given in the numerical phase diagram. These differences in phase diagram can be attributed to the different values of parameter γ and the high accuracy projection method employed in our calculations. When γ is finite, the contribution of higher-harmonics should be taken into account in stabilizing the ordered structures. Meanwhile, the projection method has the capability of

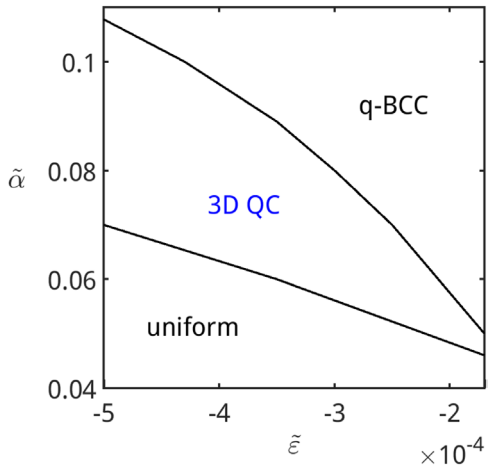

Figure 7. $\tilde{\varepsilon} - \tilde{\alpha}$ phase diagram of the model system (1) for finite γ. The ratio of two characteristic length $q = 1/(2\cos(\pi/5))$. The region labeled 'uniform' indicates that the homogeneous state is globally stable.

obtaining the contribution. Irrespective of whether γ is finite or infinite, the 3D QC is a global stable phase in the model system equation (1) with two characteristic length scales. It also should be pointed out that when ε is positive and large enough, the 2-, and 10-fold ordered structures have been predicted to be stable [28].

4. Conclusion

In summary, we investigated the emergence and stability of 3D icosahedral quasicrystals in a simple free energy functional with two characteristic length scales. In the model system, the two characteristic length scales are contained in the interaction potential function. When the ratio of the two length scales is set at the golden ratio, we predicted that the 3D icosahedral quasicrystals to be stable both for γ infinite and finite using the BMA method and a high-precision numerical method, the projection method. These results provide a good understanding of the rich phase behaviour contained in the two characteristic length scale systems. More significantly, this work extends the nonlinear resonant mechanism from 2D to 3D that the interactions between Fourier modes of densities at two length scale can stabilize the quasicrystals. This work can be helpful for further studying more complex soft-matter systems such as block copolymers and soft particles with multi-length-scale interactions.

Acknowledgments

The work is supported by the National Science Foundation of China (Grant No. 11401504, 21274005, 11421101, 11421110001, and 91430213). KJ would like to thank the financial supported by the Youth Project Hunan Provincial Education Department of China (Grant No. 16B257). ACS acknowledges the support from the Natural Sciences and Engineering Research Council (NSERC) of Canada.

Reference

[1] Meyer Y 1972 *Algebraic Numbers and Harmonic Analysis* (Amsterdam: North-Holland)
[2] Shechtman D, Blech I, Gratias D and Cahn J W 1984 *Phys. Rev. Lett.* **53** 1951
[3] Tsai A P 2008 *Sci. Technol. Adv. Mater.* **9** 013008
[4] Steurer W 2004 *Z. Kristallogr.* **219** 391
[5] Zeng X, Ungar G, Liu Y, Percec V, Dulcey A E and Hobbs J K 2004 *Nature* **428** 157
[6] Percec V, Imam M R, Peterca M, Wilson D A and Heiney P A 2009 *J. Am. Chem. Soc.* **131** 1294
[7] Percec V, Imam M R, Peterca M, Wilson D A, Graf R, Spiess H W, Balagurusamy V S K and Heiney P A 2009 *J. Am. Chem. Soc.* **131** 7662
[8] Hayashida K, Dotera T, Takano A and Matsushita Y 2007 *Phys. Rev. Lett.* **98** 195502
[9] Zhang J and Bates F S 2012 *J. Am. Chem. Soc.* **134** 7636
[10] Gillard T M, Lee S and Bates F S 2016 *Proc. Natl Acad. Sci. USA* **113** 201601692
[11] Fischer S, Exner A, Zielske K, Petrich J, Deloudi S, Steurer W, Lindner P and Förster S 2011 *Proc. Natl Acad. Sci. USA* **108** 1810
[12] Talapin D V, Shevchenko E V, Bodnarchuk M I, Ye X, Chen J and Murray C B 2009 *Nature* **461** 964
[13] Janot C 1992 *Quasicrystals: a Primer* (Oxford: Oxford University Press)
[14] Steurer W and Deloudi S 2009 *Crystallography of Quasicrystals: Concepts, Methods and Structures* (Berlin: Springer)
[15] Hiller H 1985 *Acta Crystallogr.* A **41** 541
[16] Henley C L, de Boissieu M and Steurer W 2006 *Phil. Mag.* **86** 1131
[17] Lifshitz R and Diamant H 2007 *Phil. Mag.* **87** 3021
[18] Leibler L 1980 *Macromolecules* **13** 1602
[19] Mermin N D and Troian S M 1985 *Phys. Rev. Lett.* **54** 1524
[20] Müller H W 1994 *Phys. Rev.* E **49** 1273
[21] Lifshitz R and Petrich D M 1997 *Phys. Rev. Lett.* **79** 1261
[22] Silber M, Topaz C M and Skeldon A C 2000 *Physica* D **143** 205
[23] Dotera T 2007 *Phil. Mag.* **87** 3011
[24] Barkan K, Diamant H and Lifshitz R 2011 *Phys. Rev.* B **83** 172201
[25] Archer A J, Rucklidge A M and Knobloch E 2013 *Phys. Rev. Lett.* **111** 165501
[26] Barkan K, Engel M and Lifshitz R 2014 *Phys. Rev. Lett.* **113** 098304
[27] Jiang K, Tong J and Zhang P 2016 *Commun. Comput. Phys.* **19** 559
[28] Jiang K, Tong J, Zhang P and Shi A-C 2015 *Phys. Rev.* E **92** 042159
[29] Subramanian P, Archer A J, Knobloch E and Rucklidge A M 2016 *Phys. Rev. Lett.* **117** 075501
[30] Quandt A and Teter M P 1999 *Phys. Rev.* B **59** 8586
[31] Skibinsky A, Buldyrev S V, Scala A, Havlin S and Stanley H E 1999 *Phys. Rev.* E **60** 2664
[32] Dotera T and Gemma T 2006 *Phil. Mag.* **86** 1085
[33] Engel M and Trebin H-R 2007 *Phys. Rev. Lett.* **98** 225505
[34] Reinhardt A, Romano F and Doye J P K 2013 *Phys. Rev. Lett.* **110** 255503
[35] Jiang K and Zhang P 2014 *J. Comput. Phys.* **256** 428
[36] MCarley J S and Ashcroft N W 1994 *Phys. Rev.* B **49** 15600
[37] Alexander S and McTague J 1978 *Phys. Rev. Lett.* **41** 702
[38] Bak P 1985 *Phys. Rev. Lett.* **54** 1517
[39] Dotera T, Oshiro T and Ziherl P 2014 *Nature* **506** 208
[40] Zappa E, Dykeman E C, Geraets J A and Twarock R 2016 *J. Phys. A: Math. Theor.* **49** 175203
[41] Nesterov Y 2013 *Introductory Lectures on Convex Optimization: a Basic Course* (Berlin: Springer)
[42] Silber M and Proctor M R E 1998 *Phys. Rev. Lett.* **81** 2450
[43] Chaikin P M and Lubensky T C 1995 *Principles of Condensed Matter Physics* (Cambridge: Cambridge University Press) ch 4.7